Molecular Crystals and Liquid Crystals
Publication details, including instructions for authors and subscription information:
http://www.tandfonline.com/loi/gmcl20

Dielectric and Electrooptic Studies of Chiral Thioester

M. Marzec [a], M. Bohdan [a], M. D. Ossowska-Chruściel [b], J. Chruściel [b] & S. Wróbel [a]

[a] Institute of Physics, Jagiellonian University, Kraków, Poland

[b] Institute of Chemistry, University of Natural Science and Humanities, Siedlce, Poland

Version of record first published: 14 Jun 2011

To cite this article: M. Marzec, M. Bohdan, M. D. Ossowska-Chruściel, J. Chruściel & S. Wróbel (2011): Dielectric and Electrooptic Studies of Chiral Thioester, Molecular Crystals and Liquid Crystals, 540:1, 227-238

To link to this article: http://dx.doi.org/10.1080/15421406.2011.568889

Mol. Cryst. Liq. Cryst., Vol. 540: pp. 227–238, 2011

ISSN: 1542-1406 print/1563-5287 online
DOI: 10.1080/15421406.2011.568889

Taylor & Francis
Taylor & Francis Group

Dielectric and Electrooptic Studies of Chiral Thioester

M. MARZEC,[1] M. BOHDAN,[1] M. D. OSSOWSKA–CHRUŚCIEL,[2] J. CHRUŚCIEL,[2] AND S. WRÓBEL[1]

[1]Institute of Physics, Jagiellonian University, Kraków, Poland
[2]Institute of Chemistry, University of Natural Science and Humanities, Siedlce, Poland

The aim of this work is to study by complementary methods physical properties of calamitic chiral thioester showing ferroelectric behaviour. Phase transition temperatures, stability as well as rich polymorphism have been investigated by DSC measurements and texture observations. The type of the paraelectric–ferroelectric phase transition has been studied based on the spontaneous polarization measurements. The relaxation processes have been revealed in all liquid crystalline phases and sub-phases using the dielectric spectroscopy method. The interpretation of all of them is presented.

Keywords Dielectric relaxation; ferroelectric phase; spontaneous polarization; sub-phases

1. Introduction

One of the very interesting and unexpected properties of liquid crystals is the ferroelectricity found by Meyer et al. [1] as well as the antiferroelectricity discovered by Chandani et al. [2]. Those and several subsequent phenomena have been intensively studied, and took effect in their practical application (e.g., LCD). Learning of the ferroelectric and antiferroelectric phases as well as the sub-phases occurring between them are essential in understanding their intrinsic properties.

Typical phase sequence during cooling of chiral liquid crystalline substance being of MHPOBC analogue is as follows: $SmA^* - SmC^*_\alpha - SmC^* - SmC^*_\beta - SmC^*_\gamma - SmC^*_A$, which was predicted by a discrete phenomenological model solution [3–5]. The SmC^*_α sub-phase is a clock structured with short period of helix, typically from 5 to a 50 smectic layers [6–13]. This sub-phase appears always below paraelectric SmA^* phase and shows up as an antiferroelectric one in its high temperature range and ferroelectric one in its low temperature range [14]. The SmC^*_β sub-phase is a clock structured sub-phase [15] as well but for many years it used to be considered as the ferroelectric SmC^* phase. On the other hand in several studies it was shown that this sub-phase exhibits antiferroelectric properties [16–18] for the

Address correspondence to M. Marzec, Institute of Physics, Jagiellonian University, Reymonta 4, Kraków, Poland. Tel.: +48 12 663 5549; E-mail: Monika.Marzec@uj.edu.pl

optically very pure compounds. There has been also shown in the end that the SmC^*_β sub-phase is earlier found the SmC^*_{FI2} sub-phase (denoted also as AF or SmC^*_{AF}). However, the SmC^* phase shows up when the purity of the compounds decreases [19]. Its pseudo-unit cell consists of four layers. The SmC^*_γ sub–phase (denoted also as SmC^*_{FI1}) is also clock structured one, but it exhibits ferrielectric properties, which is a result of the non cancelled polarization over the three-layered periodicity [20].

The aim of this work is to study physical properties of the tenth homologue of three-ring chiral thioester series n.OPOSMH which exhibits all phases and sub-phases mentioned above. The substance 10.OPOSMH has been subjected to complementary methods such as calorimetric, electrooptic measurements and dielectric spectroscopy as well. The main goal was to investigate its substantial properties such as spontaneous polarization value, collective and molecular dynamics and order of the para-ferroelectric phase transition. Interpretation of the nature of dielectric processes detected in the liquid crystalline phases will be discussed in detail.

2. Experimental

Complementary methods have been used to study physical properties of chiral calamitic tioester (S)-(+)-4-[(4-{[1-methyl]heptylcarboxyl}phenyl)-carbonylthio]phenyl-4′-decyloxy-1-benzencarboxylate (in short 10.OPOSMH). The molecular structure of the substance studied [21] is presented in Figure 1.

The substance 10.OPOSMH exhibits rich polymorphism with sub-phases: narrow SmC^*_α, and SmC^*_β and SmC^*_γ, as well as wide temperature range ferroelectric SmC^* and antiferroelectric SmC^*_A phases. The complementary methods such as differential scanning calorimetry (DSC), spontaneous polarization measurements and frequency domain dielectric spectroscopy (FDDS) have been used to study its physical properties. DSC measurements have been done using Perkin Elmer Pyris 1 DSC calorimeter and the texture observations using Nikon Eclipse polarizing microscope. To check the stability of the substance and to detect the weak transitions the 11 rates of heating and cooling (1, 3, 5, 7, 10, 15, 20, 25, 30, 35, 40 K/min) were used in the DSC measurements. Additionally, the texture observations with and without aligning electric field applied, have been performed to recognize the liquid crystalline phases during heating and cooling.

Measurements of the spontaneous polarization P_S have been done by reversal current method versus temperature for different frequencies of the triangular wave applied (5, 10, 20, 50, 100 Hz). The liquid crystalline sample was sandwiched into cell with ITO electrodes, covered by polymer layer facilitating the planar alignment. Linkam GS350 hot stage has been used for temperature controlling.

Dielectric spectra have been taken in all liquid crystalline phases during cooling of the planar aligned sample, in the broad frequency range: from 40 Hz to 10 MHz. The commercial cell (AWAT Company) of thickness of 5 μm with golden electrodes

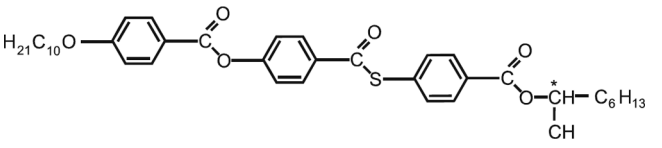

Figure 1. Molecular structure of substance 10.OPOSMH.

has been used in this case and the perpendicular component of the dielectric permittivity $\varepsilon^*_\perp(\omega) = \varepsilon'_\perp(\omega) - i\varepsilon''_\perp(\omega)$ has been measured [22]. These measurements have been done using dielectric spectrometer based on Agilent 4294A impedance analyzer.

3. Results and Discussion

3.1. *Calorimetric Measurements*

Studies of the phase transitions as well as substance stability have been carried out by DSC method and texture observations. As mentioned above the measurements have been done for 11 heating and cooling rates, but only for two rates equal to 3 K/min and 1 K/min the richest polymorphism has been observed. The curves registered for other rates show clearly only two phase transitions: melting and clearing point on heating, and clearing and crystallization on cooling. As an example the DSC curve for 1 K/min is shown in Figure 2. For each anomaly observed on DSC curves the onset temperature has been calculate and plotted versus cooling/heating rate to obtain the transition temperature at the so-called zero rate by fitting straight line to these dependences. Outcomes for heating are as follows: 80°C for melting and 150°C for clearing points; for cooling: 62°C and 150°C, respectively.

3.2. *Texture Observations*

Texture observations have been performed versus temperature without and with AC field to identify the liquid crystalline phases as well as to measure the transition temperatures. Characteristic textures for particular phase and sub-phase registered without AC field during cooling are presented in Figure 3. The phase sequences during

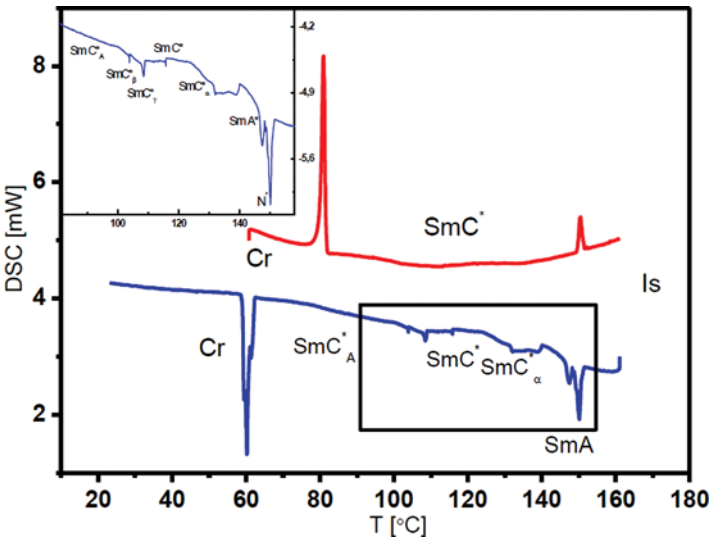

Figure 2. DSC curves at heating (red curve) and cooling (blue curve) obtained at rate equal to 1 K/min. The inset shows enlarged area of cooling curve (temperature from isotropic to SmC^*_A phase). (Figure appears in color online.)

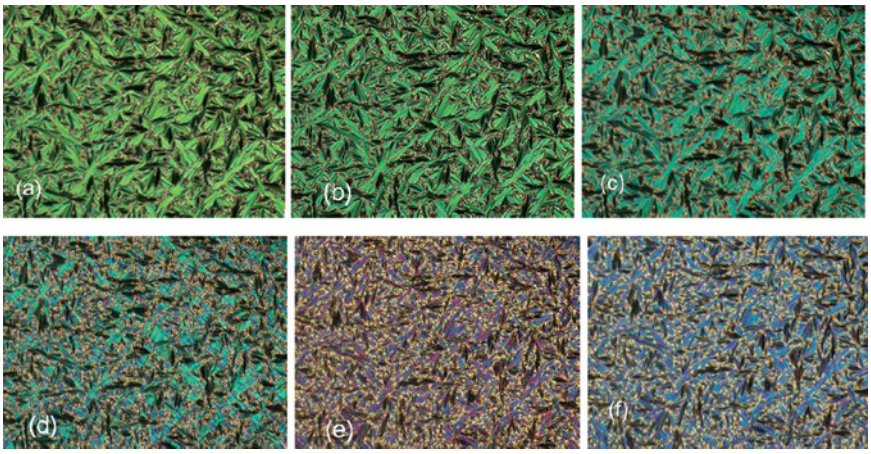

Figure 3. The textures taken without AC field in: (a) SmA* phase, (b) SmC^*_α sub-phase, (c) SmC* phase, (d) SmC^*_β sub-phase, (e) SmC^*_γ sub-phase, and (f) SmC^*_A phase. (Figure appears in color online.)

heating and cooling have been obtained taking into account the results of texture observation and DSC studies (onset temperatures):
Heating:

$$\text{Cr.}80^\circ\text{C}\ \text{SmC}^*_\text{A}116^\circ\text{C}\ \text{SmC}^*129^\circ\text{C}\ \text{SmA}^*150^\circ\text{C}\ \text{I}.$$

Cooling:

$$\text{I}150^\circ\text{C}\,\text{SmA}^*130^\circ\text{C}\,\text{SmC}^*_\alpha128^\circ\text{C}\,\text{SmC}^*116^\circ\text{C}\,\text{SmC}^*_\beta114^\circ\text{C}\,\text{SmC}^*_\gamma104^\circ\text{C}\,\text{SmC}^*_\text{A}62^\circ\text{C}\,\text{Cr}.$$

As mentioned above texture observations have been also performed with electric field of amplitude equal to 80 Vp-p. Such high voltage has been chosen because in the antiferreoelctric SmC^*_A phase the switching has been observed at this value of voltage applied. During cooling with the AC field the dark area between electrodes (Fig. 4a) has been observed in the whole temperature range of paraelectric SmA* phase what was interpreted as homeotropic texture of this phase. It means that the dielectric anisotropy of the SmA* phase is positive at low frequencies. Such reorientation of molecules under electric field applied is known in literature as Freedericks transition. During further cooling with AC field at the transition temperature to the SmC^*_α sub-phase the reorientation into the planar alignment has been

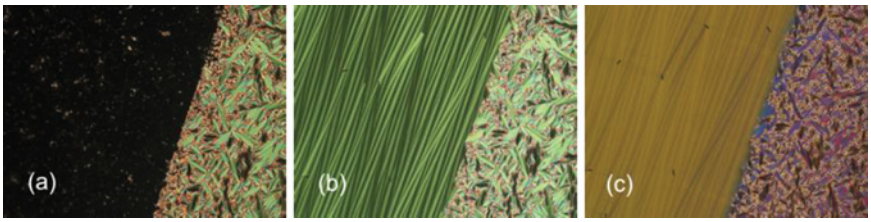

Figure 4. The textures obtained with AC aligning field in: (a) SmA* phase, (b) SmC^*_α sub-phase, and (c) SmC^*_A phase. (Figure appears in color online.)

observed and as the result the mono-domain of the SmC^*_α, ferroelectric SmC^* and antiferroelectric SmC^*_A phases, as well as SmC^*_β and SmC^*_γ sub-phases between them, have been obtained. As examples the planar textures of mono-domains are presented for the SmC^*_α sub-phase and SmC^*_A phase in Figures 4b,c.

3.3. *Spontaneous Polarization Measurements*

Measurements of the spontaneous polarization P_S have been done by reversal current method versus temperature for different frequencies of the triangular wave applied. Temperature dependence of spontaneous polarization taken at frequency $\nu = 10$ Hz is shown, as an example, in Figure 5. As one can see the SmA^* – SmC^* phase transition is continuous one and the mean field function $P_S = P_0(T_C - T)^\beta$ [23] fitted to the experimental points gives β parameter equal to 0.31. For all other frequencies of the triangular wave applied the temperature behaviour is similar and the β parameter is in range from 0.26 to 0.3. Therefore one can conclude that a tri-critical point has been observed at the transition SmA^* – SmC^*_α – SmC^*. The maximum value of P_S is equal to ca. 90 nC/cm^2 for all frequencies of driving voltage used. It is a medium value of spontaneous polarization which may mean that permanent dipole moments of two thioester groups are compensated. Four permanent dipole moments in the molecule facilitate reach polymorphism.

3.4. *Dielectric Measurements*

The aim of the dielectric studies was to find the dielectric permittivity of molecular relaxation processes appearing in the liquid crystalline phases and sub-phases. Therefore the dielectric spectra during cooling, in whole liquid crystalline

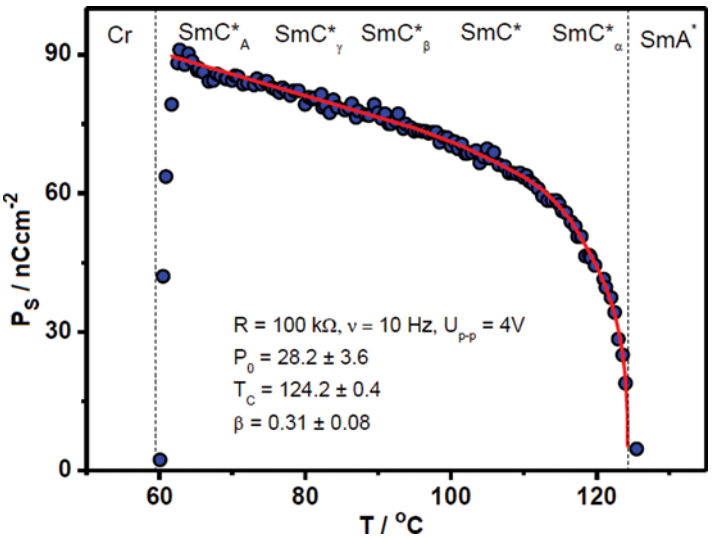

Figure 5. Temperature dependence of spontaneous polarization obtained for frequency of triangular wave applied equal to 5 Hz. The red line has been obtained by fitting the mean field function to the experimental data close to the critical temperature.

temperature range have been taken and Cole–Cole formula with conductivity and electrode polarization terms [24] has been fitted to the experimental data:

$$\varepsilon^*(\nu) = \varepsilon(\infty) + \frac{\varepsilon(0) - \varepsilon(\infty)}{1 + (i2\pi\nu\tau)^{1-\alpha}} - \frac{iA}{\varepsilon_0 \nu^M} + \frac{B}{\nu^N} \tag{1}$$

where, $\varepsilon(\infty)$ is dielectric permittivity at high frequency, $\varepsilon(0)$ dielectric permittivity at low frequencies, ν – frequency, τ – relaxation time, α – distribution parameter of relaxation process and A, B – constant. The third part is related to ionic conductivity $\sigma = 2A\pi\varepsilon_0$ while the last term is connected with electrode polarization. This model has been chosen to compute the contribution of conductivity and electrode polarization to the dielectric spectra. It is worth to point out here that the effect of high frequency losses related to low conductivity of ITO layer [25] can be neglected because the cell with golden electrodes have been used for the dielectric measurements. The critical frequency, the dielectric increment and the distribution parameter α have been obtained as fitting parameters. As examples the dielectric spectra and Cole–Cole diagrams taken in each liquid crystalline phase and sub-phase are presented in Figures 6–9. One relaxation process has been revealed in the paraelectric SmA* phase (Fig. 6) with strongly temperature dependent relaxation frequency as

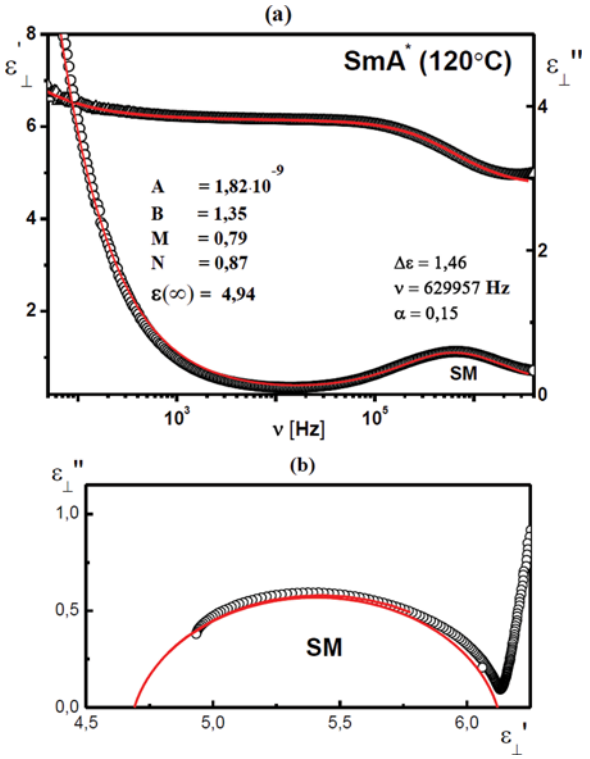

Figure 6. Dielectric spectrum (a) and Cole–Cole diagram (b) for SmA* phase. The solid line is a result of fitting Cole–Cole formula to the experimental data.

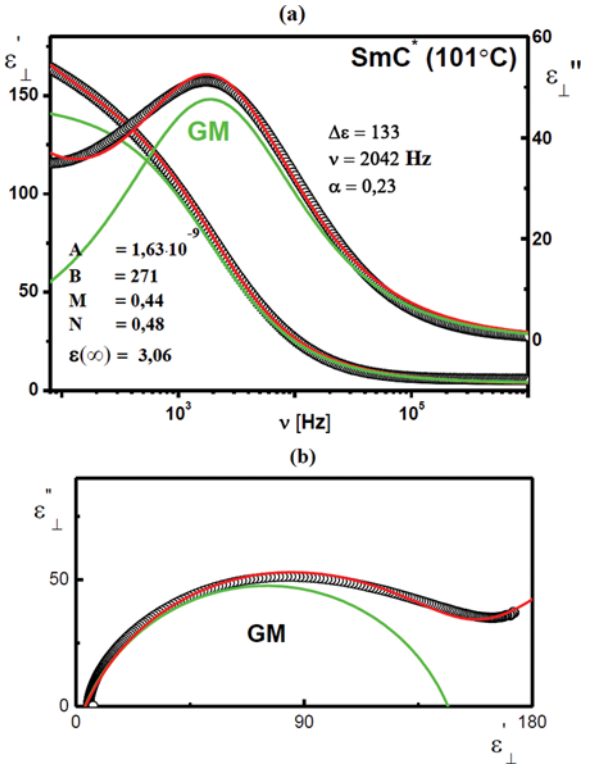

Figure 7. Dielectric spectrum (a) and Cole–Cole diagram (b) for SmC* phase. The solid line is a result of fitting Cole–Cole formula to the experimental data.

well as dielectric increment. One relaxation process has been also observed in the ferroelectric SmC* phase (Fig. 7) but this process, being almost temperature independent, appears in the low frequency range (critical frequency is equal to ca. 2 kHz) and it exhibits a large dielectric strength, ca. 130. Figure 8 presents the dielectric spectrum taken in the SmC^*_γ sub-phase with three processes visible. During further cooling, the antiferroelectric SmC^*_A phase has been revealed with characteristic dielectric spectrum consisting of two processes (Fig. 9). To identify these relaxation processes the critical frequency has been plotted versus temperature, as it is shown in Figure 10. Based on the temperature behaviour of critical frequency and dielectric increment one can interpret, according to predictions by the mean field model [26], the dielectric process registered in paraelectric SmA* phase as the soft mode (SM) and the low frequency, temperature independent, dielectric mode observed in the ferroelectric SmC* phase as the Goldstone mode (GM).

As found in literature, when the SmC^*_α sub-phase is in the temperature range of several degrees, the slope variation of temperature dependence of the relaxation frequency is slightly different in this sub-phase than in the SmA* phase and this process is called as a ferroelectric soft mode [27–30]. Such situation seems to take place in the case of 10.OPOSMH studied (see Fig. 10).

In the antiferroelectric SmC^*_A phase there are possible four different relaxation modes connected with four various collective stochastic movements of molecules [31]: two amplitudons and two phasons. Concerning amplitudons, one can find

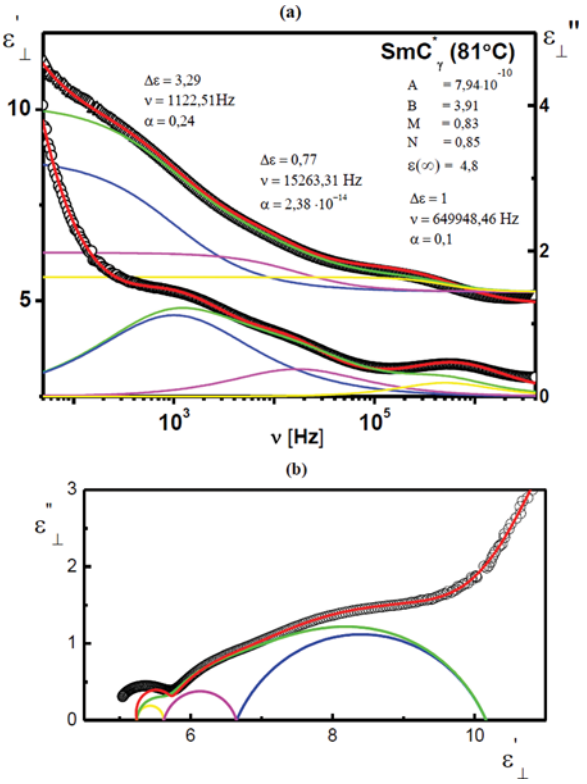

Figure 8. Dielectric spectrum (a) and Cole–Cole diagram (b) for SmC^*_γ phase. The solid line is a result of fitting Cole–Cole formula to the experimental data.

ferroelectric amplitudon connected with in-phase fluctuation of the tilt of molecules in adjacent layers and anti-phase fluctuation of the tilt of molecules in neighbouring layers called antiferroelectric amplitudon. Two phasons are as follows: antiferroelectric mode which is connecting with in-phase fluctuations of the director's phase in adjacent layers and ferroelectric one connected with anti-phase fluctuations of the director's phase in neighbouring layers. The antiferroelectric phason is sometimes called as antiferroelectric Goldstone mode because in-phase fluctuations in the same direction cost no energy, like in the case of Goldstone mode in the ferroelectric phase. On the other hand the ferroelectric phason is also called as non-cancellation mode (NCM)[32]. The ferroelectric amplitudon is also known as the soft mode in the antiferroelectric SmC^*_A phase by Yu. Panarin *et al.* [33]. From these four processes only two are polar and can be active in dielectric spectroscopy, namely ferroelectric amplitudon and ferroelectric phason [31]. Additionally, the boundary conditions, e.g. the geometry of a cell used for dielectric measurements have influence on which of the relaxation processes can be observed in the antiferroelectric SmC^*_A phase [34].

Further interpretation of the dielectric processes registered in the lower temperature phases and sub-phases could be made based on Arrhenius plot $f_C = f_0 e^{-\frac{E_a}{k_B T}}$ and calculation of activation energy. The relaxation times versus inverse of absolute temperature are shown in Figure 11. As one can see, Process 2 with activation energy

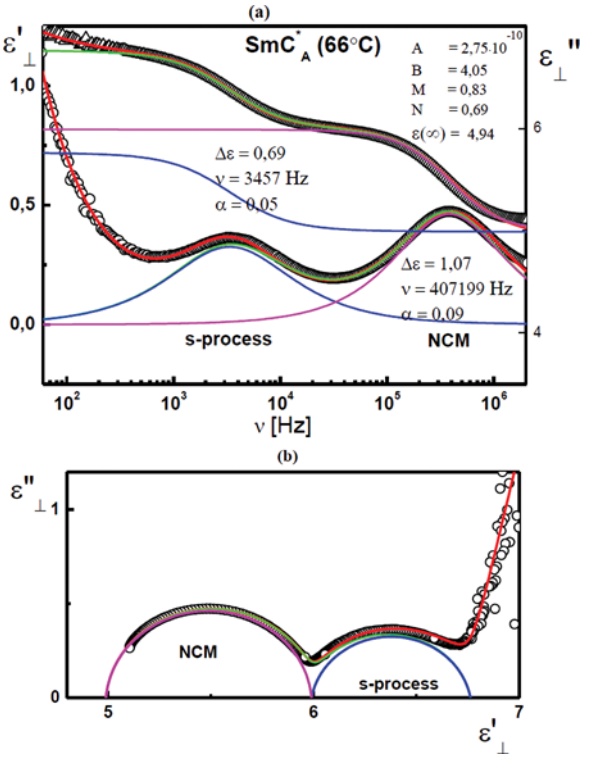

Figure 9. Dielectric spectrum (a) and Cole–Cole diagram (b) for SmC^*_A phase. The solid line is a result of fitting Cole–Cole formula to the experimental data.

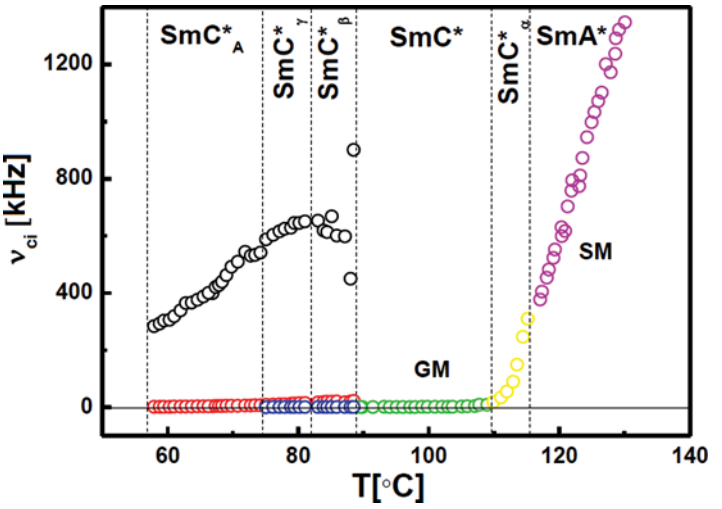

Figure 10. Temperature dependences of critical frequencies for processes revealed in all liquid crystalline phases.

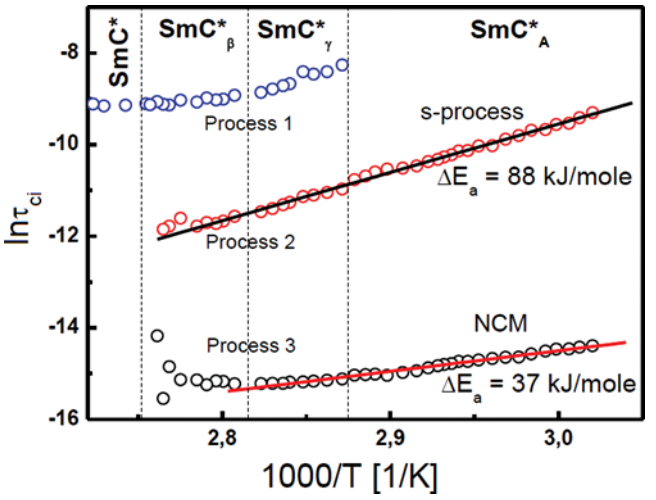

Figure 11. Arrhenius plot for all relaxation processes revealed in the SmC^*_A phase and SmC^*_β and SmC^*_γ sub-phases.

equal to 88 kJ/mole is visible in the SmC^*_β, SmC^*_γ sub-phases as well as in SmC^*_A phase and doesn't change at the phase transition. The value of activation energy of this process suggests that it could be connected with the reorientation of molecule around the short axis (s-process), as it was observed by different authors [32,35,36]. On the other hand, the process denoted as Process 3 in Figure 11, registered in frequencies close to 1 MHz, with activation energy equal to $E_a = 37$ kJ/mole, could be interpreted as a non-cancelation mode (NCM) in antiferroelectric SmC^*_A, what is in good agreement with the results obtained by other authors [32,37,38] This process is resulting from incomplete compensation of polarization in the neighboring layers [39]. The Process 1 registered in low frequency range in the SmC^*_β and SmC^*_γ sub-phases, is comparable with the Goldstone mode in ferroelectric phase but is slightly temperature dependent. Some authors interpreted such process in the SmC^*_γ sub-phase as a ferrielectric Goldstone mode [40–42]. On the other hand Cepic *et al.* interpreted this low frequency process as to be related to the movements of domain boundaries [43]. From another point of view the process registered in the SmC^*_β sub-phase was interpreted as anti-phase reorientation of the director with constant tilt [42]. Summarizing, in this study a proper interpretation of this low frequency process seems to be as follows: it is connected with in-phase fluctuation of phase, which looks a little bit different in the SmC^*_γ and SmC^*_β sub-phases because the structure of them exhibits three-layer and four layer periodicity, respectively.

4. Conclusions

- Rich polymorphism, phase transition temperatures as well as stability of 10.OPOSMH substance have been found by DSC measurements and texture observations.
- The spontaneous polarization measurements in the vicinity of the critical temperature show that the paraelectric–ferroelectric phase transition is neither a second nor a first order. It seems to be a tri-critical point.

- Using dielectric spectroscopy measurements and data analyzing the relaxation processes have been revealed in the liquid crystalline phases, namely: soft mode (SM) in the paraelectric SmA^* phase as well as in the SmC^*_α sub-phase and Goldstone Mode (GM) in the whole temperature range of the ferroelectric SmC^* phase. Three processes have been observed in the sub-phases SmC^*_β and SmC^*_γ and two in the SmC^*_A phase. One of them has been interpreted as molecular process S and the second one as non-cancelation mode (NCM) in all these phases mentioned above. The third process in the SmC^*_β and SmC^*_γ sub-phases seems to be connected with in-phase fluctuation of azimuthal angle, which slightly differ in these sub-phases because they differ in the structure.

Acknowledgments

The research was carried out with the equipment purchased thanks to the financial support of the European Regional Development Fund in the framework of the Polish Innovation Economy Operational Program (contract no. POIG.02.01.00-12-023/08). The Polish State Committee for Scientific Research (KBN) is gratefully acknowledged for financial support in scope of the grant No. N N202 076435.

References

[1] Meyer, R. B., Liébert, L., Strzelecki, L., & Keller, P. (1975). *J. Phys., France*, *36*, L69.
[2] Chandani, A. D. L., Górecka, E., Ouchi, Y., Takezoe, H., & Fukuda, A. (1989). *Jap. J. Appl. Phys.*, *28*, L1265.
[3] Žekš, B., Blinc, R., & Čepič, M. (1991). *Ferroelectrics*, *122*, 221.
[4] Žekš, B., & Čepič, M. (1993). *Liquid Crystals*, *14*, 445.
[5] Čepič, M., & Žekš, B. (1995). *Mol. Cryst. Liq. Cryst.*, *263*, 61.
[6] Skarabot, M., Cepic, M., Zeks, B., Blinc, R., Heppke, G., Kityk, A. V., & Musevic, I. (1998). *Phys. Rev. E*, *58*, 575.
[7] Mach, P., Pindak, R., Levelut, A. M., Barois, P., Nguyen, H. T., Baltes, H., Hird, M., Toyne, K., Seed, A., Goodby, J. W., Huang, C. C., & Furenlidy, L. (1999). *Phys. Rev. E*, *60*, 6793.
[8] Schlauf, D., Bahr, C., & Nguyen, H. T. (1999). *Phys. Rev. E*, *60*, 6816.
[9] Laux, V., Isaert, N., Faye, V., & Nguyen, H. T. (2000). *Liq. Cryst.*, *27*, 81.
[10] Olson, D. A., Pankratz, S., Johnson, P. M., Cady, A., Nguyen, H. T., & Huang, C. C. (2001). *Phys. Rev. E*, *63*, 061711.
[11] Cady, A., Olson, D. A., Han, X. F., Nguyen, H. T., & Huang, C. C. (2002). *Phys. Rev. E*, *65*, 030701.
[12] Cady, A., Han, X. F., Olson, D. A., Orihara, H., & Huang, C. C. (2003). *Phys. Rev. Lett.*, *91*, 125502.
[13] Huang, C. C., Liu, Z. Q., Cady, A., Pindak, R., Caliebe, W., Barois, P., Nguyen, H. T., Ema, K., Takekoshi, K., & Yao, H. (2004). *Liquid Crystals*, *31*, 127.
[14] Lagerwall, J. P. F. (2005). *Phys. Rev. E*, *71*, 051703.
[15] Takezoe, H., Lee, J., Chandani, A. D. L., Gorecka, E., Ouchi, Y., & Fukuda, A. (1991). *Ferroelectrics*, *114*, 187.
[16] Li, J. F., Shack, E. A., Yu, Y. K., Wang, X. Y., Rosenblatt, C., Neubert, M. E., Keats, S. S., & Gleeson, H. (1996). *Jpn. J. Appl. Phys.*, *35*, L1608.
[17] Sako, T., Kimura, Y., Hayakawa, R., Okabe, N., & Suzuki, Y. (1996). *Jpn. J. Appl. Phys.*, *35*, L114.

[18] Jakli, A. (1999). *J. Appl. Phys.*, *85*, 1101.
[19] Gorecka, E., Pociecha, D., Cepic, M., Žekš, B., & Dabrowski, R. (2002). *Phys. Rev. E*, *65*, 061703.
[20] Takezoe, H., Gorecka, E., & Cepic, M. (2010). *Rev. Mod. Phys.*, *82*, 897–937.
[21] Ossowska-Chruściel, M. D. (2007). *Phase Transitions*, *80*, 757.
[22] Marzec, M., Mikułko, A., Wróbel, S., & Haase, W. (2007). *Dielectric Properties of Liquid Crystals*, Galewski, Z. & Sobczyk, L. (Eds.), Transworld Research Network: India, Chapter 4.
[23] Blinc, R., Heppke, G., Kityk, A. V., & Muševič, I. (1998). *Phys. Rev. E*, *58*, 575.
[24] Kresse, H. (2003). *Relaxation Phenomena*, Wróbel, S. & Haase, W. (Eds.), Springer-Verlag: Berlin Heidelberg, Chapter 5.7, 400.
[25] Perkowski, P. (2009). *Opto–Electronics Rev.*, *17*(2), 180–186.
[26] Blinc, R., & Žekš, B. (1978). *Phys. Rev. A*, *18*, 740.
[27] Kimura, Y., & Hayakawa, R. (2002). *Eur. Phys. J. E.*, *9*, 3.
[28] Cepic, M., Heppke, G., Hollidt, J. M., Lotzsch, D., Moro, D., & Zeks, B. (1995). *Mol. Cryst. Liq. Cryst.*, *263*, 207.
[29] Sarmento, S., Carvalho, P. S., Chaves, M. R., Nguyen, H. T., & Pinto, F. (1999). *Mol. Cryst. Liq. Cryst.*, *328*, 457.
[30] Pandey, M. B., Dhar, R., Agrawal, V. K., Dabrowski, R., & Tykarska, M. (2004). *Liquid Crystals*, *31*, 973–987.
[31] Muševič, I., Blinc, R., & Žekš, B. (2000). *The Physics of Ferroelectric and Antiferroelectric Liquid Crystals*, World Scientific Publishing Co. Pte. Ltd.: Singapore.
[32] Legrand, Ch., Douali, R., Dubois, F., & Nguyen, H. T. (2003). *Relaxation Phenomena*, Haase, W. & Wróbel, S. (Eds.), Springer-Verlag: Berlin Heidelberg, Chapter 5.10, 480.
[33] Panarin, Yu. (2003). *9th FLC 2003 Tutorial*, Dublin.
[34] Rudquist, P., Lagerwall, J. P., Meier, J. G., D'havé, K., & Lagerwall, S. T. (2002). *Phys. Rev. E*, *66*, 061708.
[35] Panarin, Yu. P., Kalinovskaya, O., & Vij, J. K. (1998). *Liquid Crystals*, *25*, 241–252.
[36] Marzec, M., Ganzke, D., Haase, W., Dąbrowski, R., Fąfara, A., & Wróbel, S. (2001). *Mol. Cryst. Liq. Cryst.*, *366*, 583–591.
[37] Makrenek, M., Ganzke, D., Haase, W., Wróbel, S., & Dąbrowski, R. (2001). *Mol. Cryst. Liq. Cryst.*, *366*, 573–581.
[38] Fąfara, A., Marzec, M., Wróbel, S., Dąbrowski, R., & Haase, W. (2001). *IEEE Transactions on Dielectrics and Electrical Insulation*, *8*(3), 477–480.
[39] Mikułko, A., Douali, R., Legrand, Ch., Marzec, M., Wróbel, S., & Dąbrowski, R. (2005). *Phase Transition*, *78*, 905.
[40] Merino, S., de la Fuente, M. R., Gonzalez, Y., Jubindo, M. A., Ros, B., & Puertolas, J. (1996). *Phys. Rev. E*, *54*, 5169.
[41] Panarin, Yu. P., Kalinosvskaya, O., & Vij, J. K. (1997). *Phys. Rev. E*, *55*, 4345.
[42] Wojciechowski, M., Gromiec, L. A., & Bak, G. W. (2006). *J. Mol. Liquids*, *124*, 7.
[43] Cepic, M., Gorecka, E., Pociecha, D., Zeks, B., & Nguyen, H. T. (2002). *J. Chem. Phys.*, *117*, 1817.